Microcavities integrated in metal halide perovskite light-emitting field-effect transistors

Results in Physics 44 (2023) 106168

Contents lists available at ScienceDirect

Results in Physics

journal homepage: www.elsevier.com/locate/rinp

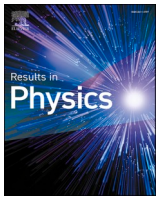

Microcavities integrated in metal halide perovskite light-emitting field-effect transistors

Francesco Scotognella

Dipartimento di Fisica, Politecnico di Milano, Piazza Leonardo da Vinci 32, 20133 Milano, Italy

ARTICLE INFO

Keywords:
Metal halide perovskite
Light-emitting transistor
Photonic microcavities
Transfer matrix method

ABSTRACT

Metal halide perovskites are materials that show unique characteristics for photovoltaics and light emission. Amplified spontaneous emission and stimulated emission has been shown with these materials, together with electroluminescence in light-emitting diodes and light-emitting transistors. An important achievement that combine stimulated emission and electroluminescence could be the fabrication of electrically driven metal halide perovskite lasers.

In this work, the integration of metal halide perovskite light-emitting field-effect transistors with photonic microcavities is proposed. This can lead to the engineering of electrically driven lasers. The microcavities have been designed in order to have the cavity mode at 750 nm, which is the peak wavelength of the electroluminescent spectrum of recently reported $MaPbI_3$-based electroluminescent devices. The optical properties of the photonic microcavities have been simulated by means of the transfer matrix method, considering the wavelength dependent refractive indexes of all the materials involved. The material for the gate is indium tin oxide, while different materials, either inorganic or organic, have been considered for the microcavity architectures.

Introduction

Metal halide perovskites show ground-breaking properties in terms of photovoltaic efficiency and light emission [1]. In April 2021, a power conversion efficiency of 25.6 % has been reached with a perovskite solar cell [2]. In July 2022, 31.25 % efficiency for tandem perovskite-silicon solar cell has been achieved [3]. Concerning light emission, metal halide perovskite based light emitting diodes are very established [4,5]. Furthermore, amplified spontaneous emission and laser emission has been observed in many reports with metal halide perovskites [6–8]. The very recent review by Liu et al. [9] reports different types of optically pumped metal halide perovskite laser cavities, such as whispering gallery mode (WGM), Fabry-Pérot, vertical cavity surface emitting laser (VCSEL). Outstanding laser performances have been achieved, with very low lasing threshold. It is noteworthy that a $CsPbBr_3$ quantum dot based VCSEL has shown laser emission at 522 nm with a linewidth of 0.9 nm and an ultralow lasing threshold of 0.39 $\mu J/cm^2$ [10]. With $MAPbI_3$ thin films, laser emission at longer wavelengths has been achieved. For example, with a $MAPbI_3$ thin film based VCSEL, laser emission has been shown at 778 nm, with a linewidth of 0.2 nm and a laser threshold of 7.6 $\mu J/cm^2$ [11]. The combination of laser emission and electroluminescence is very challenging, but it can lead to the fabrication of electrically driven perovskite lasers, a breakthrough for many applications from photonics to communications. Interesting structures are proposed to achieve such device [12].

The use of light-emitting field-effect transistors could be strategic for electrically driven lasing, since they allow a high carrier density together with the control of current flow, charge injection and emission patterns [13,14]. The ambipolar characteristics of metal halide perovskites, such as methylammonium lead iodide (CH3NH3PbI3 or MAPbI3), allow the fabrication of MAPbI3-based light-emitting transistors [15–17]. The integration of a laser cavity in light-emitting diodes could be pursued via the inclusion of photonic crystals in the transistors. Organic light-emitting transistors with photonic crystal gate dielectrics have been proposed in previous reports [18,19], demonstrating electroluminescence spectral modulation and enhancement.

In this work, we have designed different microcavities integrated with light-emitting field effect transistors based on metal halide perovskites. These architectures could allow the fabrication of electrically driven metal halide perovskite lasers in which the microcavities provide the feedback mechanism. Different materials are employed to widen the fabrication possibilities: inorganic materials such as silicon dioxide, titanium dioxide, fluorine indium co-doped cadmium oxide (FICO), silicon; organic polymers as polyvinyl carbazole (PVK), cellulose acetate

E-mail address: francesco.scotognella@polimi.it.

https://doi.org/10.1016/j.rinp.2022.106168
Received 6 August 2022; Received in revised form 9 September 2022; Accepted 7 December 2022
Available online 10 December 2022

(CA). The transfer matrix method has been employed considering all the wavelength dependent refractive indexes of the materials.

Methods

In this work the transmission spectra of the microcavities have been simulated with the transfer matrix method, a well establish tool to study-one dimensional photonic structures [20,21]. Within this method the matrix used for the *k*th layer is given by

$$M_k = \begin{bmatrix} cos\left(\frac{2\pi}{\lambda}n_k(\lambda)d_k\right) & -\frac{i}{n_k(\lambda)}sin\left(\frac{2\pi}{\lambda}n_k(\lambda)d_k\right) \\ -in_k(\lambda)sin\left(\frac{2\pi}{\lambda}n_k(\lambda)d_k\right) & cos\left(\frac{2\pi}{\lambda}n_k(\lambda)d_k\right) \end{bmatrix} \quad (1)$$

with $n_k(\lambda)$ the wavelength dependent refractive index of the layer and d_k the thickness of the layer (in nm). The matrix describing the whole multilayer system is given by the product of the M_k matrices

$$M = \prod_{i=1}^{N} M_k = \begin{bmatrix} M_{11} & M_{12} \\ M_{21} & M_{22} \end{bmatrix} \quad (2)$$

The integer number N represents the number of layers. From the matrix elements of the matrix M it is possible to compute the transmission coefficient

$$t = \frac{2n_s}{(M_{11} + M_{12}n_0)n_s + (M_{21} + M_{22}n_0)} \quad (3)$$

and, consequently, the transmission

$$T = \frac{n_0}{n_s}|t|^2 \quad (4)$$

In Eqs. (4) and (5), n_0 and n_s are the refractive indexes of air and glass, respectively.

For silicon dioxide, the following Sellmeier equation has been employed [22,23]

$$n^2_{SiO_2}(\lambda) - 1 = \frac{0.6961663\lambda^2}{\lambda^2 - 0.0684043^2} + \frac{0.4079426\lambda^2}{\lambda^2 - 0.1162414^2} + \frac{0.8974794\lambda^2}{\lambda^2 - 9.896161^2} \quad (5)$$

For titanium dioxide, the wavelength-dependent refractive index is given by [24]

$$n_{TiO_2}(\lambda) = \left(4.99 + \frac{1}{96.6\lambda^{1.1}} + \frac{1}{4.60\lambda^{1.95}}\right)^{1/2} \quad (6)$$

For PVK, the Sellmeier equation for the refractive index of is given by [25,26]:

$$n^2_{PVK}(\lambda) - 1 = \frac{0.09788\lambda^2}{\lambda^2 - 0.3257^2} + \frac{0.6901\lambda^2}{\lambda^2 - 0.1419^2} + \frac{0.8513\lambda^2}{\lambda^2 - 1.1417^2} \quad (7)$$

For CA, the Sellmeier equation for the refractive index of CA is [25,26]:

$$n^2_{CA}(\lambda) - 1 = \frac{0.6481\lambda^2}{\lambda^2 - 0.0365^2} + \frac{0.5224\lambda^2}{\lambda^2 - 0.1367^2} + \frac{2.483\lambda^2}{\lambda^2 - 13.54^2} \quad (8)$$

In the Eqs. (5) to (8) λ is in micrometers.

To predict the behaviour of the plasmonic response in our photonic structures the Drude model can be employed [27,28], where the frequency dependent complex dielectric function of ITO and FICO can be written as:

$$\varepsilon_{FICO}(\omega) = \varepsilon_1(\omega) + i\varepsilon_2(\omega) \quad (9)$$

where

$$\varepsilon_1 = \varepsilon_\infty - \frac{\omega_P^2}{(\omega^2 - \Gamma^2)} \quad (10)$$

and

$$\varepsilon_2 = \frac{\omega_P^2\Gamma}{\omega(\omega^2 - \Gamma^2)} \quad (11)$$

with

$$\omega_P = \sqrt{\frac{Ne^2}{\varepsilon_0 m^*}} \quad (12)$$

For ITO $N = 2.49 \times 10^{26} cm^{-3}$, $\varepsilon_\infty = 4$, $m^* = 0.4m_e$ and $\Gamma = 0.1132eV$ [29]. For FICO $N = 1.68 \times 10^{27} cm^{-3}$, $\varepsilon_\infty = 5.6$, $m^* = 0.43m_e$ and $\Gamma = 0.07eV$ [29,30].

The wavelength dependent refractive index of silicon is taken from Ref. [31]. Considering the studied wavelength range for the microcavity that includes silicon layers (500 – 1500 nm), the imaginary part of the refractive index is neglected. Finally, the wavelength dependent refractive of the active material $MAPbI_3$ is taken from Refs. [32,33]. Such refractive index dispersion includes the real part and the imaginary part.

Results and discussion

The typical structure of a light-emitting transistor integrated with a microcavity is depicted in Fig. 1, in agreement with the structures fabricated in Refs. [18,19]. As gate contact, indium tin oxide has been selected following the transistor design reported in Ref. [19]. Such material is interesting is interesting for light-emitting devices because of its transparency in the visible range. The source and drain contacts are placed at the two sides of the $MaPbI_3$ layer. Several materials can be used as source and drain, such as gold/nickel [15] or gold/titanium [34].

For all the microcavities studied in this work, the selected thickness for the $MaPbI_3$ layer is 40 nm, as reported in the fabrication of a $MAPbI_3$-based light-emitting diode [5]. To tune the thickness of the defect, the $MaPbI_3$ layer is embedded between two layers of another material. In the example in Fig. 1, the two one dimensional photonic crystals are made of titanium dioxide and FICO, while the $MaPbI_3$ layer is embedded between two layers of silicon dioxide. The employment of FICO is interesting since it could allow also the possibility of UV light-induced dielectric function change via photodoping [30].

In Fig. 2 the transmission spectrum of the structure depicted in Fig. 1 is shown. The one-dimensional photonic crystals have six bilayers of TiO_2 and FICO. The cavity mode with the highest transmission is centred at 750 nm, where previously reported $MAPbI_3$-based light-emitting diodes show the peak wavelength of the electroluminescent spectrum

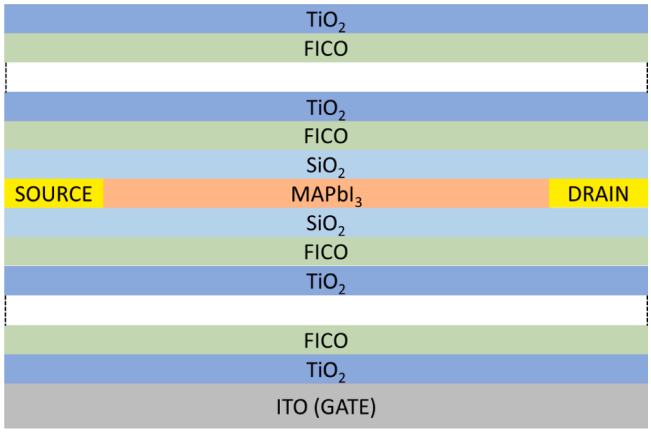

Fig. 1. Structure of the $MaPbI_3$ light-emitting field-effect transistor integrated with a microcavity composed by two FICO/TiO_2 one-dimensional photonic crystals with the $MaPbI_3$ layer as defect.

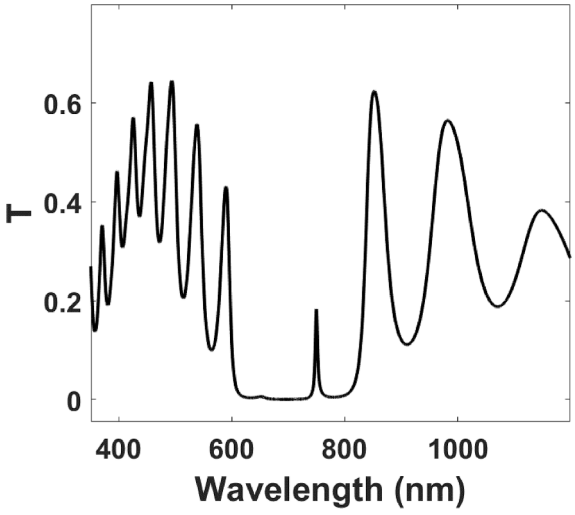

Fig. 2. Transmission spectrum of ITO/$(TiO_2/FICO)_6/SiO_2/MaPbI_3/SiO_2/(FICO/TiO2)_6$.

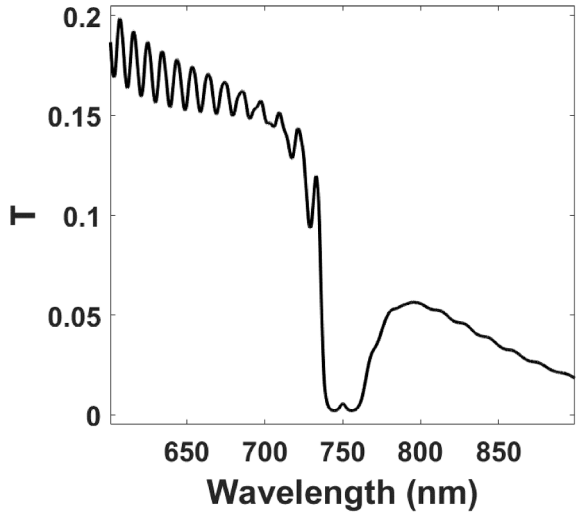

Fig. 4. Transmission spectrum of ITO/$(SiO_2/FICO)_{50}/TiO_2/MaPbI_3/TiO_2/(FICO/SiO_2)_{50}$.

[5,12]. The microcavity shows an additional cavity mode at 652 nm, very weak in terms of transmission.

The thickness of the ITO layer is 100 nm. The thickness of the titanium dioxide layers is 73.5 nm, while the thickness of the FICO layers is 112.7 nm. With 6 bilayers of TiO_2 and FICO, the total thickness of each photonic crystal is 1117 nm. In order to have the cavity mode at 750 nm, the $MaPbI_3$ layer is embedded between two layers of silicon dioxide with a thickness of 144.2 nm. In this structure, the weaker defect mode at 652 nm is more evident.

Since the photonic crystal between the ITO-based gate and the active material, i.e. $MaPbI_3$, has to act as a gate dielectric, its thickness is crucial for the operation of the light-emitting transistor. Moreover, also the thickness silicon dioxide buffer layer within the cavity should be considered.

The thickness can be controlled with the number of bilayers in the photonic crystals. With 4 bilayers of TiO_2 and FICO, the total thickness of each photonic crystal is 745 nm (Fig. 3), in line with the thickness employed in a previously reported light-emitting transistor [19].

A microcavity in which the one-dimensional photonic crystal is made of SiO_2 and FICO and the defect is made of $TiO_2/MaPbI_3/TiO_2$ shows a transmission spectrum as in Fig. 4. The thickness of the silicon dioxide layers is 128.4 nm, while the thickness of FICO is 124.1 nm. The thickness of the titanium dioxide layers is 139.5 nm. Because of the similar real part of the refractive index of silicon dioxide and FICO, the photonic band gap is relatively narrow and a high number of bilayers is needed to achieve a sufficiently efficient photonic band gap. Because of the high number of layers of FICO the transmission strongly decreases in the near infrared.

To achieve very thin photonic crystals, and thus a very thin gate dielectric ITO and $MaPbI_3$, a structure alternating silicon dioxide and silicon is designed (Fig. 5). The thickness of the silicon layers is 53.1 nm, while the thickness of the silicon dioxide layers is 123.9 nm. The thickness of the titanium dioxide layers in the microcavity defect is 139.5 nm. Thus, the total thickness of the dielectric between ITO and $MaPbI_3$ is 493.5 nm. This thickness of 493.5 nm is very promising for the realization of high performing metal halide light-emitting transistors, since such value is in line with the dielectric thicknesses reported in Refs. [15–17].

Finally, a microcavity with fully organic photonic crystals has been designed, allowing completely different fabrication techniques such as spin coating (Fig. 6) [35]. The two one-dimensional photonic crystals are made of PVK and CA. With these two materials, the refractive index

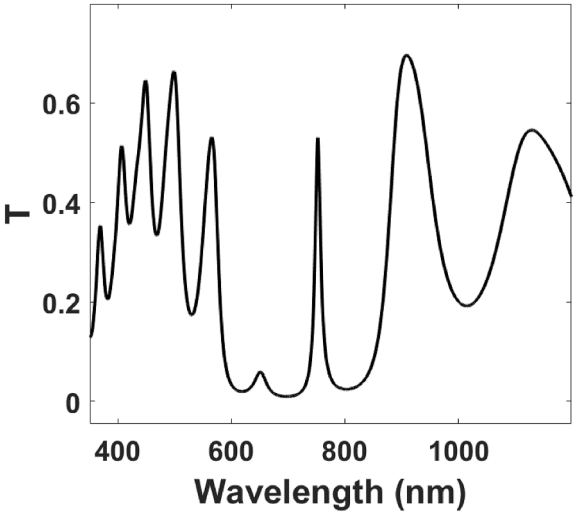

Fig. 3. Transmission spectrum of ITO/$(TiO_2/FICO)_4/SiO_2/MaPbI_3/SiO_2/(FICO/TiO2)_4$.

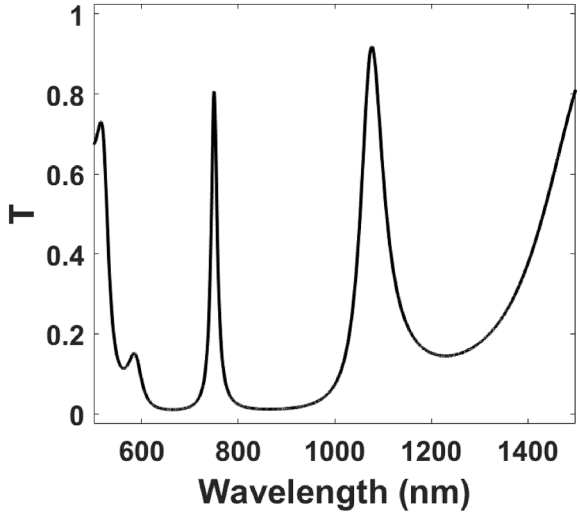

Fig. 5. Transmission spectrum of ITO/$(SiO_2/Si)_2/TiO_2/MaPbI_3/TiO_2/(Si/SiO_2)_2$.

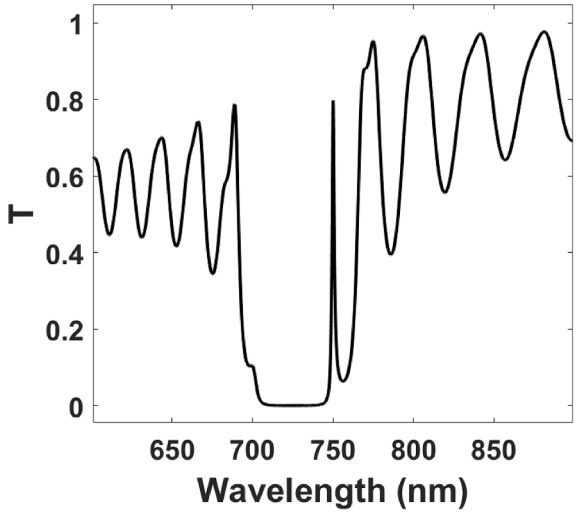

Fig. 6. Transmission spectrum of ITO/$(CA/PVK)_{25}$/CA/$MaPbI_3$/CA/$(PVK/CA)_{25}$.

is quite high for polymers. However, to achieve an efficient photonic band gap, a high number of bilayers is needed.

Conclusion

Different microcavities integrated with metal halide based light-emitting field-effect transistors have been designed by means of transfer matrix method. Different materials have been employed in order to provide a library of diverse architectures. The architectures include ITO as gate dielectric and the active material $MaPbI_3$ is embedded between two one-dimensional photonic crystals. The photonic crystals have been made with silicon, silicon dioxide, titanium dioxide, FICO, PVK and CA. With the couple Si/SiO_2, very thin photonic crystals have been engineered. These architectures, that are compatible with $MAPbI_3$-based light-emitting transistors [15–17] and $MAPbI_3$-based VCSELs [11] reported in literature, could allow the fabrication of electrically driven metal halide perovskite lasers.

Declaration of Competing Interest

The authors declare that they have no known competing financial interests or personal relationships that could have appeared to influence the work reported in this paper.

Data availability

Data will be made available on request.

Acknowledgement

This project has received funding from the European Research Council (ERC) under the European Union's Horizon 2020 research and innovation programme (grant agreement No. [816313]).

References

[1] Sun J, Wu J, Tong X, Lin F, Wang Y, Wang ZM. Organic/inorganic metal halide perovskite optoelectronic devices beyond solar cells. Adv Sci 2018;5:1700780. https://doi.org/10.1002/advs.201700780.
[2] Jeong J, Kim M, Seo J, Lu H, Ahlawat P, Mishra A, et al. Pseudo-halide anion engineering for α-FAPbI3 perovskite solar cells. Nature 2021;592:381–5. https://doi.org/10.1038/s41586-021-03406-5.
[3] E. Bellini, CSEM, EPFL achieve 31.25% efficiency for tandem perovskite-silicon solar cell, Pv Magazine International. (n.d.). https://www.pv-magazine.com/2022/07/07/csem-epfl-achieve-31-25-efficiency-for-tandem-perovskite-silicon-solar-cell/ (accessed July 26, 2022).
[4] Kumawat NK, Gupta D, Kabra D. Recent advances in metal halide-based perovskite light-emitting diodes. Energy Technol 2017;5:1734–49. https://doi.org/10.1002/ente.201700356.
[5] Zhao L, Roh K, Kacmoli S, Al Kurdi K, Jhulki S, Barlow S, et al. Thermal management enables bright and stable perovskite light-emitting diodes. Adv Mater 2020;32:2000752. https://doi.org/10.1002/adma.202000752.
[6] Deschler F, Price M, Pathak S, Klintberg LE, Jarausch D-D, Higler R, et al. High photoluminescence efficiency and optically pumped lasing in solution-processed mixed halide perovskite semiconductors. J Phys Chem Lett 2014;5:1421–6. https://doi.org/10.1021/jz5005285.
[7] Cegielski PJ, Giesecke AL, Neutzner S, Porschatis C, Gandini M, Schall D, et al. Monolithically integrated perovskite semiconductor lasers on silicon photonic chips by scalable top-down fabrication. Nano Lett 2018;18:6915–23. https://doi.org/10.1021/acs.nanolett.8b02811.
[8] Alvarado-Leaños AL, Cortecchia D, Folpini G, Kandada ARS, Petrozza A. Optical gain of lead halide perovskites measured via the variable stripe length method: what we can learn and how to avoid pitfalls. Adv Opt Mater 2021:2001773. https://doi.org/10.1002/adom.202001773.
[9] A. Liu, G. Guan, X. Chai, N. Feng, M. Lu, X. Bai, Y. Zhang, Metal halide perovskites toward electrically pumped lasers. Laser Photon Rev n/a (n.d.) 2200189. 10.1002/lpor.202200189.
[10] Huang L, McCormick TM, Ochi M, Zhao Z, Suzuki M-T, Arita R, et al. Spectroscopic evidence for a type II Weyl semimetallic state in MoTe 2. Nat Mater 2016;15:1155–60. https://doi.org/10.1038/nmat4685.
[11] Chen S, Zhang C, Lee J, Han J, Nurmikko A. High-Q, low-threshold monolithic perovskite thin-film vertical-cavity lasers. Adv Mater 2017;29:1604781. https://doi.org/10.1002/adma.201604781.
[12] Gao W, Yu SF. Reality or fantasy—Perovskite semiconductor laser diodes. EcoMat 2021;3:e12077.
[13] Prosa M, Moschetto S, Benvenuti E, Zambianchi M, Muccini M, Melucci M, et al. 2,3-Thienoimide-ended oligothiophenes as ambipolar semiconductors for multifunctional single-layer light-emitting transistors. J Mater Chem C 2020;8:15048–66. https://doi.org/10.1039/D0TC03326J.
[14] Chen H, Huang W, Marks TJ, Facchetti A, Meng H. Recent advances in multi-layer light-emitting heterostructure transistors. Small 2021;17:2007661. https://doi.org/10.1002/smll.202007661.
[15] Chin XY, Cortecchia D, Yin J, Bruno A, Soci C. Lead iodide perovskite light-emitting field-effect transistor. Nat Commun 2015;6:7383. https://doi.org/10.1038/ncomms8383.
[16] Maddalena F, Chin XY, Cortecchia D, Bruno A, Soci C. Brightness enhancement in pulsed-operated perovskite light-emitting transistors. ACS Appl Mater Interfaces 2018;10:37316–25. https://doi.org/10.1021/acsami.8b11057.
[17] Klein M, Li J, Bruno A, Soci C. Co-evaporated perovskite light-emitting transistor operating at room temperature. Adv Electron Mater 2021;7:2100403. https://doi.org/10.1002/aelm.202100403.
[18] Namdas EB, Hsu BBY, Yuen JD, Samuel IDW, Heeger AJ. Optoelectronic gate dielectrics for high brightness and high-efficiency light-emitting transistors. Adv Mater 2011;23:2353–6. https://doi.org/10.1002/adma.201004102.
[19] Natali M, Quiroga SD, Passoni L, Criante L, Benvenuti E, Bolognini G, et al. Simultaneous tenfold brightness enhancement and emitted-light spectral tunability in transparent ambipolar organic light-emitting transistor by integration of high-k photonic crystal. Adv Funct Mater 2017;27:1605164. https://doi.org/10.1002/adfm.201605164.
[20] M. Born, E. Wolf, A.B. Bhatia, P.C. Clemmow, D. Gabor, A.R. Stokes, A.M. Taylor, P.A. Wayman, W.L. Wilcock, Principles of optics: electromagnetic theory of propagation, interference and diffraction of light, 7th ed., Cambridge University Press, 1999. 10.1017/CBO9781139644181.
[21] Bellingeri M, Chiasera A, Kriegel I, Scotognella F. Optical properties of periodic, quasi-periodic, and disordered one-dimensional photonic structures. Opt Mater 2017;72:403–21. https://doi.org/10.1016/j.optmat.2017.06.033.
[22] Malitson IH. Interspecimen comparison of the refractive index of fused silica*,†. J Opt Soc Am JOSA 1965;55:1205–9. https://doi.org/10.1364/JOSA.55.001205.
[23] RefractiveIndex.INFO - Refractive index database, (n.d.). https://refractiveindex.info/ (accessed November 15, 2019).
[24] F. Scotognella, A. Chiasera, L. Criante, E. Aluicio-Sarduy, S. Varas, S. Pelli, A. Łukowiak, G.C. Righini, R. Ramponi, M. Ferrari, Metal oxide one dimensional photonic crystals made by RF sputtering and spin coating. Ceram Int. 41 (2015) 8655–8659. 10.1016/j.ceramint.2015.03.077.
[25] Fornasari L, Floris F, Patrini M, Comoretto D, Marabelli F. Demonstration of fluorescence enhancement via Bloch surface waves in all-polymer multilayer structures. Phys Chem Chem Phys 2016;18:14086–93. https://doi.org/10.1039/C5CP07660A.
[26] Manfredi G, Mayrhofer C, Kothleitner G, Schennach R, Comoretto D. Cellulose ternary photonic crystal created by solution processing. Cellul 2016;23:2853–62. https://doi.org/10.1007/s10570-016-1031-x.
[27] Müller J, Sönnichsen C, von Poschinger H, von Plessen G, Klar TA, Feldmann J. Electrically controlled light scattering with single metal nanoparticles. Appl Phys Lett 2002;81:171. https://doi.org/10.1063/1.1491003.
[28] Novotny L, Hecht B. Principles of nano-optics. 2. ed. Cambridge: Cambridge Univ. Press; 2012.
[29] Kriegel I, Scotognella F, Manna L. Plasmonic doped semiconductor nanocrystals: Properties, fabrication, applications and perspectives. Phys Rep 2017;674:1–52. https://doi.org/10.1016/j.physrep.2017.01.003.
[30] Kriegel I, Urso C, Viola D, De Trizio L, Scotognella F, Cerullo G, et al. Ultrafast photodoping and plasmon dynamics in fluorine-indium codoped cadmium oxide nanocrystals for all-optical signal manipulation at optical communication

wavelengths. J Phys Chem Lett 2016;7:3873–81. https://doi.org/10.1021/acs.jpclett.6b01904.
[31] Schinke C, Christian Peest P, Schmidt J, Brendel R, Bothe K, Vogt MR, et al. Uncertainty analysis for the coefficient of band-to-band absorption of crystalline silicon. AIP Adv 2015;5:067168. https://doi.org/10.1063/1.4923379.
[32] Phillips LJ, Rashed AM, Treharne RE, Kay J, Yates P, Mitrovic IZ, et al. Dispersion relation data for methylammonium lead triiodide perovskite deposited on a (100) silicon wafer using a two-step vapour-phase reaction process. Data Brief 2015;5:926–8. https://doi.org/10.1016/j.dib.2015.10.026.
[33] Phillips LJ, Rashed AM, Treharne RE, Kay J, Yates P, Mitrovic IZ, et al. Maximizing the optical performance of planar CH3NH3PbI3 hybrid perovskite heterojunction stacks. Sol Energy Mater Sol Cells 2016;147:327–33. https://doi.org/10.1016/j.solmat.2015.10.007.
[34] Park B. Probing and passivating electron traps at the MAPbI3/TiO2 interface. Results Phys 2021;23:104025. https://doi.org/10.1016/j.rinp.2021.104025.
[35] Komikado T, Yoshida S, Umegaki S. Surface-emitting distributed-feedback dye laser of a polymeric multilayer fabricated by spin coating. Appl Phys Lett 2006;89:061123. https://doi.org/10.1063/1.2336740.